Microalgal-driven pH changes in the boundary layer lead to apparent increases in Pb internalization by a unicellular alga in the presence of citrate.

Paula Sánchez-Marín[1,2], Fengjie Liu[1], Zhongzhi Chen[1,3], Claude Fortin[1] and Peter G.C. Campbell[1]

E-mail addresses:

Paula Sánchez-Marín: paulasanchez@uvigo.es

Fengjie Liu: fengjie.liu@ete.inrs.ca

Zhongzhi Chen: Zhongzhi.chen@h2oinnovation.com

Claude Fortin: claude.fortin@ete.inrs.ca

Peter G.C. Campbell: peter.campbell@ete.inrs.ca

Present addresses:

[1] Institut National de la Recherche Scientifique, Centre Eau Terre Environnement (INRS-ETE), 490 rue de la Couronne, Québec, QC, Canada G1K 9A9

[2] Department of Ecology and Animal Biology and ECIMAT, University of Vigo, 36310 Vigo, Galicia, Spain

[3] H_2O Innovation, 330 rue St-Vallier Est, Suite 340, Québec, QC, Canada G1K 9C5

Running header: "Boundary-layer pH affects algal uptake of Pb"

Abstract

Several cases have been described in the literature where different ligands enhanced lead (Pb) bioavailability over what would have been expected on the basis of equilibrium models such as the biotic ligand model (BLM). These exceptions compromise the development of BLMs for this metal, and mechanistic knowledge of the involved processes is still insufficient. The present study shows that the hydrophilic organic ligand citrate enhances Pb internalization by *Chlamydomonas reinhardtii* for both the wild and the wall-less strains. Despite the high Pb internalization fluxes shown by this alga, which may be near the limits set by diffusion through the boundary layer, and its capacity to assimilate citrate (and potentially Pb-citrate complexes), neither of these mechanisms could quantitatively account for the observed increase in Pb internalization in the presence of this ligand. However, algal-driven pH increases in the boundary layer and concomitant changes in Pb speciation successfully explained the observed results. This study suggests that information on bulk solution chemistry is not enough to predict metal bioavailability for organisms that can substantially modify the chemical composition of their boundary layer, as observed for *C. reinhardtii.*

Keywords: microalgae, metal bioavailability, biotic ligand model, boundary layer

Introduction

Dissolved metal bioavailability towards aquatic organisms is controlled by the chemical composition of the exposure medium, as predicted by the free ion activity model (FIAM) and its derivative, the biotic ligand model (BLM). These models are based on equilibrium chemistry and on the main assumption that the metal is internalized in its cationic form after binding to a membrane-bound carrier (the biotic ligand) (Campbell 1995; Campbell and Fortin 2013; Morel 1983). The main outcome of this unified theory is that metal bioavailability, or the proportion of the biotic ligands bound to the metal, will depend on the free ion activity of the metal in the bulk solution – which will vary with ionic strength and with the presence of metal ligands – and on the concentration of other cations that can competitively bind to the same biotic ligand. On this basis, empirical biotic ligand models (BLMs) have been constructed for many metal-organism combinations (Rüdel et al. 2015). These BLMs incorporate empirically derived constants for the binding of various cations to the biotic ligand, and they can be used to predict a metal effect level (such as an EC_{50}) on the basis of free metal concentration and medium composition (Gorsuch et al. 2002; Paquin et al. 2002). Despite the recognized usefulness of this approach, mechanistic and more fundamental studies have shown in some cases that several of the implicit assumptions underlying the BLM theory are not always fulfilled in real field situations (Campbell et al. 2002; Slaveykova and Wilkinson 2005).

Several studies involving microalgae have shown different cases where metal bioavailability (i.e., uptake and/or toxicity) did not agree with BLM predictions. The most common mechanisms explaining these exceptions are: (i) the existence of non-equilibrium conditions, such as diffusive limitation of the rate of metal movement from the bulk

solution to the algal surface (Buffle et al. 2009; Fortin and Campbell 2000; Hudson 1998); (ii) uptake of hydrophobic metal-ligand complexes by diffusion through the cell membrane, effectively by-passing the usual facilitated uptake route (Phinney and Bruland 1994); (iii) uptake of hydrophilic metal-ligand complexes through a ligand carrier, usually referred to as "piggy-back uptake" (Fortin and Campbell 2001). Recent work has focused on "boundary layer" effects, which highlight the importance of considering the capacity of the algae to modify the chemistry in their immediately adjacent medium, i.e. the “phycosphere” (Liu et al. 2017). These biologically-driven changes in the physicochemical conditions of the phycosphere can cause the chemical speciation of trace elements in the boundary layer to be different from that in the bulk solution. Similar phenomena have been recognized for the roots of higher plants (Hinsinger et al. 2003) and the gills of freshwater fish (Playle et al. 1992; Playle and Wood 1989).

Although empirical BLMs have been proposed for Pb (De Schamphelaere et al. 2014; Nys et al. 2014), mechanistic studies about Pb bioavailability have revealed examples where the Pb uptake process did not follow BLM assumptions. Slaveykova and Wilkinson (2003) showed that the effect of pH on Pb^{2+} internalization by the green microalga *Chlorella kesslerii* could not be explained by considering speciation and competition effects only. The higher Pb internalization observed at high pH was explained by the authors as the result of the internalization of $PbCO_3$ or $Pb(OH)^+$ complexes by the alga, although non-competitive effects of pH on the cell membrane might partially account for the observed effects too (François et al. 2007). In a previous study, we showed that Pb internalization by *C. reinhardtii* was enhanced in the presence of dissolved inorganic carbon (DIC), and we proposed that under conditions of diffusion limitation of Pb

internalization, $PbCO_3$ complexes could contribute to this enhancement by dissociating in the boundary layer and supplying additional free Pb^{2+} ions for uptake (Sánchez-Marín et al. 2013). In the present study, we sought to extend our mechanistic knowledge of the effects of ligands on Pb bioavailability to *C. reinhardtii*, using the organic ligand citrate. The presence of citrate has been shown to increase the bioavailability of other metals to phytoplankton, such as Cd and Zn (Errécalde and Campbell 2000; Errécalde et al. 1998) or rare earth elements (Zhao and Wilkinson 2015).

In the present study, we varied the concentration of citrate under constant conditions (pH, ionic strength and competing cations) and tested the ability of the free Pb^{2+} concentration to predict Pb internalization by *C. reinhardtii*. As the results deviated from BLM predictions, several hypothesis-driven experiments were performed to find a mechanistic explanation that could account for the observed deviations.

Methods

Reagents and labware

All experimental and culture media were prepared in ultrapure water (resistivity ≥ 18 MΩ cm). Salts and other reagents used for cultures and experiments were of analytical grade or better. A concentrated analytical standard solution of Pb (Fluka analytical; 1 mg mL^{-1}), preserved in 4% HNO_3, was used to spike the experimental media. Radiolabelled citrate ([1,5-^{14}C]-citrate) was purchased from Perkin-Elmer. All plastic containers and glassware were soaked for 24 h in 10% (v/v) HNO_3 (ACS grade, Fisher Scientific), rinsed abundantly with ultrapure water, and then dried under a class 100 laminar flow hood before use.

Algae culture

Chlamydomonas reinhardtii P.A. Dangeard wild strain (CPCC11) and a wall-less strain (CPCC12) were obtained from the Canadian Phycological Culture Centre (University of Waterloo) and cultured in the low ionic strength modified high salt medium (MHSM) described by Fortin and Campbell (2000), with the only change being that KNO_3 was replaced by $NaNO_3$, and 0.01 M HEPES (4-(2-hydroxyethyl)-1-piperazine-ethanesulphonic acid) was added to buffer the pH at 7.0. Cultures were maintained at 20 ºC and constant light (100 μmol photons m^{-2} s^{-1}). Cell concentrations, size distributions and cell surface area were determined with an electronic particle counter (Multisizer 3 Coulter Counter, 70 μm aperture).

Short-term Pb uptake experiments

A simplified version of MHSM medium (SMHSM) was used to expose and rinse the algal cells; this simplified formulation excluded trace metals, phosphate and HEPES buffer. The pH of the solutions was adjusted to 7.0 ± 0.1 with additions of 0.1 M NaOH. The experimental solutions were left to equilibrate inside closed 50-mL polypropylene tubes for a minimum of 2 h before the start of the experiments. It was verified that the bulk solution pH remained constant during the equilibration and exposure period. In one of the experiments, when Pb^{2+} speciation analysis was to be performed on the water samples after the exposure period, 0.01 M HEPES was kept in the medium formulation with the aim of stabilizing the pH for a longer time, and nitrilotriacetic acid (NTA) was included as a control ligand to buffer the Pb^{2+} concentrations.

Cells in the mid-exponential growth phase (day 2 of the culture) were harvested by gentle filtration through polycarbonate filters (2-µm pore size; Millipore), washed several times with SMHSM, and resuspended in 5 mL of SMHSM. About 200 µL of the concentrated algal suspension were inoculated into the experimental solutions to obtain a cell density of 5×10^4 cells·mL^{-1}, which was determined with more exactitude in three experimental solutions only used for this purpose.

A preliminary time-course experiment was performed to check for linearity of Pb uptake with time (5 to 50 min) and to calculate uptake rates of Pb in the presence of citrate or NTA. In subsequent experiments, the algae were exposed to the experimental solutions for a fixed time (35 min). Exposure was done in a test chamber at 20 ºC and a light intensity of 100 µmol photons m^{-2} s^{-1}. After the exposure period, the algae were separated from the medium by filtration through two superimposed polycarbonate filters (2-µm pore size; Millipore); the bottom filter was used to correct for metal adsorption. After filtration, 20 mL of ethylenediamine-tetraacetic acid (EDTA) washing solution were added and left in contact with the algae for 10 min. The EDTA solution contained 1 mM Na_2EDTA, 1.6 mM NH_4NO_3 and 2 mM $NaNO_3$, and pH was adjusted to 7.0 by additions of 1 M NaOH. The algae were then washed two more times with the EDTA solution, and the still-damp filters were separated and transferred into labelled and pre-washed polypropylene vials for subsequent metal analysis.

The wall-less cells were very fragile and they broke easily during the normal filtration process. For the experiment done with this strain, gentle filtration was carried out with extra care and minimal vacuum pressure. In addition, some changes were introduced in this experiment (which was performed in parallel with the wild and the wall-less strains)

to monitor the actual number of cells being analyzed. Cells were exposed to the experimental solutions at a higher cell density (1×10^5 cells·mL^{-1}), harvested by gentle filtration and resuspended in 10 mL of EDTA washing solution. One mL of this algal suspension was taken to determine actual cell densities and the remaining 9 mL were centrifuged (2000 g, 5 min). The supernatant was withdrawn and the pellets were kept for subsequent metal analysis. The number of cells remaining in the supernatant was < 2% of the total number of cells in the vials.

Metal analysis

Vials with collected algae or filters were dried (70ºC; 24 h) and the cells were digested with concentrated HNO_3 by heating at 90 ºC for 1 h. After appropriate dilution, Pb concentrations in the digests were analyzed by inductively coupled plasma-mass spectrometry (ICP-MS: X Series; Thermo Elemental, Cheshire, UK). Lead concentrations were first calculated in μmoles Pb·cell^{-1}and then divided by the mean surface cellular area obtained from each experiment to yield units in μmoles Pb·m^{-2}.

Lead concentrations in the experimental solutions were determined in a 0.5-mL subsample taken from each treatment just before introduction of the algal cells, and, in some experiments, in the filtrates collected after the exposure period. Analyses were done by ICP-MS after appropriate dilution and acidification with HNO_3 (5% v/v).

Procedural blanks were included during the digestion and analysis and the accuracy of the ICP-MS results was checked using a certified multielement standard (catalogue number 900-Q30-100, SCP Science).

Determination of algal-driven pH changes

To test if the CPCC11 strain of *C. reinhardtii* could modify the pH of the surrounding medium, even when this medium was well buffered, cells were exposed at very high density to simplified MHSM medium prepared both in the absence and presence of pH buffer (10 mM HEPES). A preliminary experiment was run using SMHSM and a cell density of 1.3×10^6 cells·mL^{-1}. Subsequent experiments were performed in the presence of high concentrations of DIC, to avoid the depletion of DIC in solution during exposure at such high cell densities. The DIC was increased to 4 mM (by replacing $NaNO_3$ with $NaHCO_3$ while keeping ionic strength constant. Cell density was 5×10^6 cells·mL^{-1} in the experiment in the absence of HEPES and 6×10^7 cells·mL^{-1} in the experiment in the presence of HEPES.

Cells in the mid-exponential growth phase (days 2-3 of the culture) were harvested by centrifugation in polypropylene vials at 3300 g for 10 min at 20 ºC, washed twice with the test solution and the last supernatant was collected for measuring pH at time 0. The same procedure was applied to control vials with test solution in the absence of algae. Then the algal pellet was resuspended in 50 mL of test solution in 50 mL polypropylene vials. Both the vials with algae suspensions and control vials were exposed in a test chamber (20 ºC, 110-130 µmol photons m^{-2} s^{-1}), and 12 mL samples were taken at 33 and 63 min, centrifuged at 15,800 g for 10 min at 20 ºC, and pH was immediately measured in the supernatant. For the experiments in the absence of HEPES, the vials were filled nearly to the top (without head space) and the pH electrode was directly inserted into the solutions at short intervals during the first 70 min and every two hours afterwards (until a total of 7.5

h), closing the lid of the vials between measurements to minimize pH changes caused by CO_2 interchange with air. Cell density was measured in 0.1 mL subsamples.

^{14}C-citrate uptake experiments

C. reinhardtii cells (4×10^5 cells mL^{-1}) were exposed to 10^{-5} M ^{14}C-citrate at a specific activity of 8 nCi $nmol^{-1}$ in simplified MHSM at pH 7. At 3, 30 and 60 min of exposure, two 50 mL-replicates of the cell suspension were filtered through two superimposed polycarbonate filters and washed three times with 20 mL of SMHSM. The same was done with cells exposed to 10^{-5} M ^{14}C-citrate and 100 nM Pb at a single time point (60 min). The radioactivity of the filter and the filtrate were determined by liquid scintillation counting (Perkin Elmer, Tri-Carb 2910 TR) after addition of 10 mL of Ecolume scintillation cocktail (Fisher Scientific) to the filters or 15 mL of Ecolume to 5-mL aliquots of the water samples.

The amount of citrate assimilated by the algae was calculated after correction for the citrate retained on the control filters. The limit of detection was calculated as three times the standard deviation (SD) of the amount of citrate retained by six individual control filters.

Subcellular distribution experiments

The subcellular partitioning of Pb was determined for algal cells that had been exposed during 30 min to 10 nM Pb^{2+} in the absence or presence of 100 µM citrate in SMHSM buffered by 1 mM HEPES (pH 7.0, ionic strength = 0.007 $eq\cdot L^{-1}$). Exposures

were performed in triplicate in 500-mL polycarbonate Erlenmeyer flasks, at a cell density of 1.5×10^5 cells·mL^{-1}. Lead internalization was stopped by adding EDTA to the exposure medium to reach a final concentration of 1 mM. After 10 min contact with EDTA, the cells were harvested by centrifugation (20,000 *g*, 15 min, 4 °C), and washed with 10 mL of SMHSM three times by successive resuspension and centrifugation steps. This washing process was designed to remove dissolved Pb and also any EDTA, which might have affected lead partitioning during the subsequent manipulations. After the final centrifugation, the algae were resuspended in ~2 mL SMHSM to attain sufficient biomass ($> 1\times10^7$ cells·mL^{-1}) for subcellular fractionation. A small aliquot of the algal suspension was taken to determine final cell densities; 0.5 mL was taken to determine Pb internalization by intact cells and 1.5 mL were used for the subcellular fractionation. This volume of the cell suspension was transferred into 7-mL polypropylene tubes, and cells were ruptured by sonication (Branson 250, Danbury, CT) for 4 min (power = 22 W; pulse = 0.2 s/s) (Crémazy et al. 2013) at 4 ºC. Ruptured cells were transferred into 1.5-mL ultracentrifugation vials and separated by differential centrifugation into five sub-cellular fractions (debris; NaOH-resistant or granule-like particles; organelles; heat-stable proteins (HSP) and heat-denaturable proteins (HDP or enzymes) (Lavoie et al. 2009a). Pellets were digested as previously described for the algal samples and supernatants were acidified with HNO_3 (5% v/v) prior to Pb determination by ICP-MS. Lead in each subcellular fraction was expressed as the quantity of Pb per cell. Recovery of Pb obtained from the sum of the five individual fractions represented between 61% and 72% of the intracellular Pb determined in intact cells. Relative distributions were calculated on the basis of the sum of the Pb quantities in each fraction.

Pb speciation measurements and calculations

Chemical equilibrium modelling was performed with MINEQL+ 4.62 software with updated equilibrium constants (Martell and Smith 2004). The default formation constants of the software were used for the Pb-citrate and Pb-NTA species, as it had been determined previously that these constants gave Pb speciation predictions in agreement with ion selective electrode (ISE) measurements (Sánchez-Marín et al. 2013). Unless otherwise noted, Pb^{2+} concentrations in experimental solutions were calculated by chemical equilibrium modelling on the basis of ICP-MS measured values of total Pb and measured pH, together with the known concentrations of organic ligands (NTA or citrate) added and major ion chemistry.

To check for the possible effect of algal exudates on Pb speciation, free Pb^{2+} was also measured in some samples taken before and after algal exposure using a lead solid state combination ISE (Orion 9682 ionplus). The electrode was calibrated with solutions containing 1 μM Pb in 0.01 M $NaNO_3$ at pH 7.0 and increasing additions of citrate, or in the absence of citrate for total dissolved [Pb] > 1 μM. Calibrations were done over a pPb range from 10 to 5 (10^{-10} to 10^{-5} M) and the mean slope of the calibrations performed on different days was 25.8 ± 0.4 mV.

Data treatment and statistics

Uptake data were fitted to a hyperbolic equation:

$$Pb_{\text{int}} = \frac{Pb_{\max} \cdot Pb^{2+}}{K_M + Pb^{2+}} \qquad \text{(Eqn 1)}$$

where Pb_{int} is the metal internalized by the cells after an exposure time of 35 min (normalized by surface area); Pb_{max} is the asymptotic maximum for metal internalization after 35 min and K_M is the apparent half-saturation constant. For short exposure periods (e.g., 60 min), Pb fluxes are constant over time (Sánchez-Marín et al. 2013) and plots of internalized metal versus time pass through the origin. Metal fluxes can thus be estimated dividing metal internalization by the fixed exposure time. In one of the experiments bulk Pb^{2+} concentrations were much lower than the K_M, so that uptake transporters were far from saturation. For this experiment, the uptake data were fitted to a linear equation.

Significant differences between curves were tested using the extra-sum-of-squares F-test by means of global fitting (Motulsky and Christopoulos 2003). Significant differences between Pb subcellular contents or fractions were tested by a standard t-test.

Results and Discussion

Control of Pb^{2+} concentrations in the experimental solutions

The total concentrations of Pb remaining in solution after a 35-min exposure of 1×10^5 cells·mL^{-1} ranged between 91 and 98% of the initial Pb_T concentration (before algae inoculation) for both the walled and the wall-less strains.

It is known that some wall-less mutants continuously release cell-wall constituents to the medium and this can affect metal speciation in the exposure medium (Kola et al. 2004). The wall-less mutant used in the present study derives from the CW-15 mutant described in Davies and Plaskitt (1971), a type of mutant that produces minute amounts of cell wall precursors that are released to the cell exterior in vesicles (Davies and Plaskitt

1971). Measurements of Pb^{2+} with an ISE in the filtrates of exposed wall-less cells showed that the free [Pb^{2+}] after exposure ranged between 87% and 100% of the initial concentration. Therefore, under our experimental conditions, the wall-less cells did not affect bulk solution Pb^{2+} speciation substantially.

Pb internalization in the presence or absence of citrate

Results of Pb internalization after 35 min exposure to different Pb^{2+} concentrations in the absence or presence of citrate are shown in Figure 1a. At similar Pb^{2+} concentrations, Pb internalization was higher in the presence of citrate than in its absence (F-test; $p < 0.001$), and the difference was more important at low Pb^{2+} concentrations (< 20 nM) than for higher Pb^{2+} exposure concentrations. The higher uptake rate in the presence of citrate was confirmed in a time-course experiment, where it was observed that for cells exposed to identical Pb^{2+} concentrations (6.8 nM Pb^{2+}), the uptake rate was 1.4 ± 0.2 nmol m^{-2} min^{-1} in the presence of NTA and 3.1 ± 0.3 nmol m^{-2} min^{-1} in the presence of citrate (Figure 1b).

These results are similar to those observed in a previous study with carbonate as the ligand (Sánchez-Marín et al. 2013). In that study, we suggested that Pb internalization by *C. reinhardtii* was limited by diffusion at low Pb^{2+} concentrations, a conclusion that was supported by the contrasting behaviour of *Chlorella vulgaris*. With this latter alga, for which the Pb uptake rate was ten-times lower than for *C. reinhardtii*, carbonate did not enhance Pb^{2+} internalization. A similar situation seems to apply for *C. vulgaris* and citrate, as an earlier study (Slaveykova and Wilkinson 2002) showed that citrate did not enhance Pb uptake for this alga. We speculated that in the present study the high Pb internalization rates observed for *C. reinhardtii* are near the diffusive limit of supply of the free Pb^{2+} ions,

and that Pb-citrate complexes dissociate and contribute to the internalization flux of Pb in this species.

However, as stated in our previous study, theoretical calculations of diffusive fluxes do not support this hypothesis unless we force the diffusion coefficient of Pb^{2+} to be ~ 60 times lower than the commonly accepted value for diffusion in dilute aqueous solution (Sánchez-Marín et al. 2013). Such a reduction in the diffusion constant would be plausible if the extracellular matrix of the cell wall represented a medium through which diffusion is 'restrained'(Wilkinson and Buffle 2004). Based on this reasoning, and with the aim of detecting a possible effect of the cell wall on the transport and/or uptake process, we tested if the observed effect of citrate on Pb internalization also occurred for the wall-less mutant.

Pb internalization in the presence or absence of citrate for a wall-less mutant

In order to check the differences in the effect of citrate on Pb internalization by a walled and a wall-less mutant of *C. reinhardtii*, the internalization experiment was repeated with both strains in parallel. In this case, Pb internalization in the presence of citrate was compared with Pb internalization in the presence of NTA, as this strong ligand contributes sufficient buffering capacity to allow Pb^{2+}-ISE measurements, which could not be performed in unbuffered solutions at $[Pb^{2+}] < 1$ μM (Sánchez-Marín et al. 2013).

The wall-less mutant used in this study was described as being identical to the wild type in other aspects of cell physiology except for the incapacity of producing a cell wall (Macfie et al. 1994), and the available literature suggested that both the wild and the wall-less strains CPCC11 and CPCC12 should show similar internalization fluxes for Pb

(Worms et al. 2012). However, under our experimental conditions, we observed that Pb internalization fluxes were around seven times lower for the wall-less mutant than for the wild type (compare Fig. 2a with Fig. 2b). This unexpected difference prevented us from testing our hypothesis that the cell wall restrained the diffusion of metal ions, given that the uptake fluxes seemed to be influenced by other aspects of cell physiology that differ between the two strains.

On the other hand, the effect of citrate does seem to be consistent for both strains – at similar Pb^{2+} concentrations, Pb internalization in the presence of citrate exceeded that in the presence of NTA by a factor of 2.5 to 4 for the wild type and 3 to 4.5 for the wall-less strain (Fig. 2). Our initial hypothesis, that Pb uptake was limited by diffusion from the bulk solution to the algal surface and the more labile Pb-citrate complexes dissociated in the diffusion layer whereas the stronger and less labile Pb-NTA complexes did not, cannot be considered for the wall-less mutant because the internalization flux of Pb for this mutant is too far below the calculated maximum diffusive flux. Therefore, some other mechanism must be responsible for the observed enhanced Pb internalization in the presence of citrate.

Citrate assimilation by Chlamydomonas reinhardtii

In earlier work the presence of citrate was shown to result in increased internalization of Cd^{2+} by another microalga, *Pseudokirchneriella subcapitata*, formerly known as *Selenastrum capricornutum* (Errécalde and Campbell 2000; Errécalde et al. 1998). In that case, citrate was assimilated by the alga and the increased uptake of Cd was interpreted as being the result of the internalization of Cd-citrate complexes by "piggy-back" transport, i.e., by fooling the citrate anion transporter.

To test if Pb-citrate complexes could also be internalized by piggy-back transport in *C. reinhardtii*, we monitored ^{14}C-citrate assimilation by exposing this alga to 10 μM citrate in the absence or presence of 100 nM Pb over a 60-min period (Figure 3). The results show that citrate is assimilated by the algae at a rate of 0.048 amol cell^{-1} min^{-1} (or 70 μmol m^{-2} min^{-1}) per mol L^{-1} of citrate, and that the presence of 100 nM Pb did not alter this assimilation rate.

To calculate how much Pb could be internalized by piggy-back transport, we first assumed that all citrate species are taken up by the citrate transporter at the same rate. To extrapolate citrate assimilation rates to other citrate concentrations, we further assumed that the assimilation rate constant for citrate does not vary within the range of concentrations used, i.e., from 1 to 200 μM citrate, a reasonable assumption given the good agreement between our calculated constant and that reported by Zhao and Wilkinson (2015) at 0.1 μM citrate. Based on these assumptions, we calculated the amount of Pb bound to citrate that could be internalized by piggy-back transport. This quantity was added to the predicted internalization of Pb^{2+} based on the hyperbolic or linear equation fitted to the internalization data obtained in the absence of citrate. The resulting values for Pb_{int} are represented by triangles in Figs. 1a and 2a. The potential contribution of piggy-back transport to Pb internalization is insignificant compared to the observed internalization rates. We could assume, as is discussed in the previous studies with Cd and *P. subcapitata* (Errécalde and Campbell 2000), that the Pb-citrate species are preferred, i.e., that they are transported at a higher rate than other citrate species. However, this assumption seems improbable since citrate assimilation was not altered by the presence of Pb in the solution (Fig. 3). Indeed, simple calculations showed that for citrate concentrations lower than 10 μM, the molar

quantity of extra-Pb internalized in the presence of citrate was higher than the molar quantity of citrate assimilated over the same time period (supporting information, Table S4). Therefore, uptake of intact Pb-citrate complexes is clearly unable to quantitatively explain the enhanced Pb internalization observed in the presence of this ligand.

The normalized uptake fluxes of citrate (uptake flux divided by exposure concentration) by *C. reinhardtii* (70 ± 7 μL m^{-2} min^{-1}) is similar to that observed for *P. subcapitata* (56-94 μL m^{-2} min^{-1}) (Errécalde and Campbell 2000), but the rate of Cd internalization by *P. subcapitata* was much lower than the rate of Pb internalization by *C. reinhardtii* wild strain in the present study, therefore allowing differences in the interpretation of the two studies.

Analogous results were obtained for wheat exposed to Cd (Panfili et al. 2009) and Zn (Gramlich et al. 2013) in the presence of citrate in hydroponic cultures. More metal was accumulated in the wheat roots and shoots in the presence of citrate than in its absence, at the same free metal concentrations. As was the case in the present study, citrate assimilation occurred but it could not quantitatively account for the enhancement in metal accumulation if a similar rate of uptake of citrate and metal-citrate complexes was assumed. Diffusive limitation of Zn and Cd uptake was proposed as the most plausible mechanism to explain these observations, and experimental evidence was presented in the case of Zn (Gramlich et al. 2014).

Is citrate causing a physiological effect on the alga?

Given that neither diffusive limitation nor piggy-back transport provided a satisfactory explanation for the observed effects of citrate in both wild and wall-less strains, we explored other possibilities. For example, if citrate were causing a physiological effect on the algae, such as an increase in membrane permeability or an induction of additional membrane transporters capable of moving Pb across the plasmalemma, this could explain the observed effects in both strains. To test this idea, we pre-exposed the wild strain to 100 μM citrate or to a control solution (SMHSM) for 30 min; the algae were then harvested, washed with SMHSM, and exposed for another 30 min to 5 nM Pb^{2+}. We expected that if citrate were causing a physiological effect on the alga, this effect would be still evident immediately after citrate exposure. The results showed that Pb internalization was exactly the same for both pre-treatments, with Pb_{int} equal to 0.041 ± 0.005 (n = 4) μmol m^{-2} for the cells pre-exposed to a control solution and 0.042 ± 0.002 (n = 4) μmol m^{-2} for the cells pre-exposed to citrate.

Subcellular distribution of Pb in algal cells exposed in the absence or presence of citrate

Chen et al. (2013) observed that humic acids (HA) enhanced Ag uptake by *C. reinhardtii*, but the subcellular distribution showed that all the extra-Ag accumulated in the presence of HA was attributable to the cell debris fraction. This was interpreted as an increase in the amount of Ag tightly bound to the cell surface, which was not truly internalized (Chen et al. 2013). In order to determine if a similar explanation could apply

to the Pb-citrate system, the subcellular distribution of Pb was determined for cells that had been exposed to the same Pb^{2+} concentration in the absence or presence of citrate.

Algae exposed to 10 nM Pb^{2+} for 30 min accumulated most of the Pb in the cell debris fraction (64%), followed by the organelles (21%) and granules (7.4%), and a smaller fraction was associated with proteins in the cytosol (5.2% in HSP and 2.3% in HDP) (Figure 4a). It should be noted that these data should be interpreted with caution given the incomplete recovery obtained (68 ± 4%), presumably caused by the adsorption of Pb to vial walls during the multiple transfers performed. Recovery values were, however, similar for cells exposed to Pb in the absence or presence of citrate, allowing comparison of the subcellular distribution of algae exposed to each treatment. Comparison of the subcellular distribution in algae exposed to 10 nM Pb^{2+} in the absence or presence of citrate showed that the extra-Pb accumulated in the presence of citrate was not attributable to one particular cellular compartment, but was distributed within them following the same pattern as in the absence of citrate (Fig. 4b). In the presence of citrate, Pb accumulation was approximately three times higher than in its absence for all subcellular pools, although for the cytosolic compartments this difference was not statistically significant. This increase in Pb accumulation in the presence of citrate was also observed for the cell debris, which is composed of membranes, cell wall and nuclei (Lavoie et al. 2009b), and may include some metal not truly internalized but rather so tightly adsorbed to the cell surface that it resisted the EDTA wash (Crémazy et al. 2013). The presence of citrate increased the amount of Pb in the cell debris fraction but it also increased the amount of Pb internalized by the algae in a proportional manner, so, a higher adsorption of Pb to the cell surface is not a plausible explanation of the observed results.

Algal-driven pH changes in the boundary layer

Recent studies in our laboratory have highlighted the importance of biologically-mediated chemistry in the phycosphere in determining trace metal bioavailability (Liu et al. 2017). In particular, *C. reinhardtii* (strain CC1690) was shown to be able to increase the pH in the boundary layer as a result of the release of OH^- during inorganic carbon uptake for photosynthesis, when cultured with NO_3^- as the only source of N (unpublished results). For the strain used in the present study (CPCC11, using NH_4^+ as the source of N), preliminary experiments showed that the alga at high density was also able to change the pH of an unbuffered solution, increasing it slightly during the first 3 h of exposure and decreasing it afterwards (see supporting information Fig. S1). This effect likely results from a combination of photosynthesis (i.e., CO_2/HCO_3^- uptake and subsequent OH^- release) and NH_4^+ assimilation (i.e., NH_4^+ uptake and subsequent H^+ release). In the first hours, the uptake of CO_2/HCO_3^- dominates the extracellular acid-base effect; afterwards, following the depletion of DIC in the closed system, the variation in pH is primarily influenced by NH_4^+ assimilation.

On the basis of this observation, we hypothesized that during the 35-min Pb uptake experiments, the release of OH^- from DIC uptake increased the pH in the boundary layer, even in buffered solutions (some of the Pb uptake experiments were performed in the presence of 10 mM HEPES), even though this pH change was undetectable in the bulk solution. The increase in pH would affect Pb speciation at the algal interface, leading to differences between the boundary layer and the bulk solution.

To check this hypothesis, we tested the capacity of the algae to change bulk solution pH when exposed at very high cell density (100 and 1000 times higher than in uptake experiments), in solutions enriched in DIC, to avoid DIC depletion in the solution. As expected, when exposed at very high cell density and in the presence of excess of DIC, the algae were able to increase the pH of the bulk solution, even in the presence of HEPES (Figure 5). A similar increase in pH might be occurring at the boundary layer of the cells in the Pb uptake experiments. Figure 6a shows the expected variation in Pb^{2+} concentration with pH in SMHSM in the presence of citrate, NTA or in the absence of added ligands. Whereas at pH 7 the Pb^{2+} concentrations are identical for the three solutions, as the pH increases, the concentration of Pb^{2+} decreases markedly in the solution buffered with NTA or in the absence of ligand (due to the formation of $PbOH^{+}$), but in the presence of citrate this decrease is very subtle, given that the buffering capacity of citrate contributes to alleviate the decrease in Pb^{2+} caused by OH^{-} complexation. The result is a higher concentration of Pb^{2+} in the boundary layer in the presence of citrate than in its absence or in the presence of NTA as pH increases, which in turn is reflected in a higher Pb internalization rate by the algae. Additionally, pH changes in the boundary layer may also have other effects on Pb^{2+} uptake, such as competition between Pb^{2+} and H^{+} for the biotic ligand, and non-competitive effects of pH changes on the cell membrane (François et al. 2007), but those effects would be of similar magnitude in the different treatments if the algae modifies its external pH similarly as well.

To check if the apparent deviations from BLM expectations could be satisfactorily explained by pH changes in the boundary layer, we calculated the expected Pb^{2+} concentrations at different pHs in the various treatments used in the Pb uptake experiments

previously shown in Figure 1a. The best fit was observed using pH = 8 in the boundary layer (Figure 6b, circles). At this pH, internalization results no longer deviate from predictions on the basis of [Pb^{2+}] (F-test; p = 0.73). Similarly, the uptake fluxes represented in Figure 1b would be different because of the different Pb^{2+} concentration in the boundary layer, which would be (assuming a pH of 8) 2.9 nM Pb^{2+} for the "Pb + NTA" treatment and 6.1 nM Pb^{2+} for the "Pb + citrate" treatment. These correspond to similar Pb^{2+} normalized uptake fluxes (0.48 ± 0.07 L m^{-2} min^{-1} *vs.* 0.51 ± 0.05 L m^{-2} min^{-1}). For the experiment performed in the presence of HEPES (represented in Figure 2a), the data also followed predictions on the basis of the boundary layer [Pb^{2+}] if the pH was assumed to be 8 (F-test; p = 0.063) (Figure 6b, squares). A representation of the same internalization data *vs.* calculated Pb^{2+} assuming another pH in the boundary layer (e.g. pH 9) is shown in Figure S2 in Supporting Information.

The apparent increase in Pb bioavailability in the presence of citrate can therefore be explained by algal-driven increases in pH in the boundary layer, that lead to higher boundary layer Pb^{2+} concentrations in the experiments run with citrate than in those run with NTA or in the absence of added ligands.

Re-interpretation of previous studies

The capacity of *C. reinhardtii* to modify metal speciation in the phycosphere may shed light on previous studies where apparent deviations from BLM were observed. With this in mind, we calculated how changes in pH would affect Pb^{2+} speciation in experimental solutions from a previous study where the presence of DIC was shown to enhance Pb internalization by this alga (Sánchez-Marín et al. 2013). Increases in boundary layer pH

would lead to higher decreases in Pb^{2+} concentrations in the presence of high DIC in comparison with control solutions with low DIC (Figure S3, supporting information), due to the displacement in the equilibrium HCO_3^-/CO_3^{2-}, leading to higher concentration of CO_3^{2-} (and $PbCO_3$) at higher pH. Then a lower Pb internalization would be expected in the presence of a higher DIC, contrary to the observed result. Thus, the modification of boundary layer pH by *C. reinhardtii* indicates that the enhanced Pb internalization in the presence of carbonate may be even higher than previously reported.

The results of other studies may on the contrary be better explained in light of this boundary layer pH effect. For instance, a study by Zhao and Wilkinson (2015) reported that citrate enhanced the biouptake of six trivalent rare earth elements (REEs) by *C. reinhardtii* wild strain, and similar results were observed for other low molecular weight (LMW) organic ligands and one REE (Tm). As in the present study, neither the piggy-back uptake of intact complexes nor the dissociation of complexes driven by diffusive limitation could satisfactorily explain the results. The authors proposed a mechanism that involved the formation of ternary surface complexes {L-M-R} (L being the organic ligand, M the metal ion and R the biotic ligand at the cell membrane) followed by internalization of the metal only. This mechanism was also previously proposed by Aristilde et al. (2012) to explain the enhanced Zn internalization by marine phytoplankton in the presence of LMW organic ligands, and it seems to be an evolution of the ternary complex hypothesis proposed earlier by Lamelas and coworkers (Lamelas and Slaveykova 2008; Lamelas et al. 2005) to explain Pb bioavailability in the presence of humic substances. However, ternary complexes are only supposed to contribute to metal bioavailability in cases where either the whole complex (L-M) is internalized or the ternary complex contributes to metal toxicity exerted

at the binding site in the membrane (in cases where toxicity is being used to evaluate metal bioavailability). Otherwise, the formation of {L-M-R} complexes and subsequent internalization of M can be described as a ligand exchange reaction, which should not increase metal bioavailability under equilibrium conditions (Campbell 1995; Campbell et al. 2002). Using the medium composition and conditional stability constants for Tm-citrate complexes given in Zhao and Wilkinson (2015), we calculated how extracellular changes in pH would affect Tm^{3+} speciation in the boundary layer (Fig. S4). Increases in pH from 6 (in the bulk solution) to ≥ 8 in the boundary layer would lead to a higher uptake of Tm in the presence of citrate than in its absence, as observed in the study. We suggest that algal-driven changes in pH might allow reinterpretation of this - and other - studies and offer an explanation for observed disagreements with FIAM/BLM expectations of metal bioavailability that have not been satisfactorily explained until now.

Modification of external pH by microalga and other microorganisms is not uncommon (Eisensamer and Roenneberg 2004; Kühn and Raven 2008; Milligan et al. 2009), and it may have different effects on metal speciation in the boundary layer depending on the medium composition. This process may influence not only the bioavailability and toxicity of metals of ecotoxicological concern, but it may also influence the bioaccessibility of nutrients such as Fe. This represents an additional challenge in the design and interpretation of metal bioavailability studies, one that should be added to the already long list of precautions that should be taken, such as to accurately control the concentration of competing cations, pH and ionic strength in the bulk solution, or to keep metal depletion during the tests as low as possible. Advances in the measurement of pH in

the boundary layer (using microelectrodes or pH sensitive dyes) (Kühn and Raven 2008; Milligan et al. 2009) would be of great applicability in future studies.

Acknowledgements

P. Sánchez-Marín received a postdoctoral mobility grant from the Spanish Ministry of Education. Financial support was provided by the Natural Sciences and Engineering Research Council of Canada (NSERC). C. Fortin and P. G. C. Campbell are supported by the Canada Research Chairs programme.

References

Aristilde, L., Y. Xu, and F. M. M. Morel. 2012. Weak organic ligands enhance zinc uptake in marine phytoplankton. Environ. Sci. Technol. **46:** 5438-5445.

Buffle, J., K. J. Wilkinson, and H. P. van Leeuwen. 2009. Chemodynamics and bioavailability in natural waters. Environ. Sci. Technol. **43:** 7170-7174.

Campbell, P. G. C. 1995. Interactions between trace metals and aquatic organisms: A critique of the free-ion activity model, p. 45-102. *In* A. Tessier and D. R. Turner [eds.], Metal Speciation and Bioavailability in Aquatic Systems. Wiley.

Campbell, P. G. C., O. Errécalde, C. Fortin, V. P. Hiriart-Baer, and B. Vigneault. 2002. Metal bioavailability to phytoplankton - Applicability of the biotic ligand model. Comp. Biochem. Phys. C **133:** 189-206.

Campbell, P. G. C., and C. Fortin. 2013. Biotic Ligand Model, p. 237-245. *In* J. F. Férard and C. Blaise [eds.], Encyclopedia of Aquatic Ecotoxicology. Springer-Verlag.

Crémazy, A., J. L. Levy, P. G. C. Campbell, and C. Fortin. 2013. Uptake and subcellular partitioning of trivalent metals in a green alga: Comparison between Al and Sc. BioMetals **26:** 989-1001.

Chen, Z., C. Porcher, P. G. C. Campbell, and C. Fortin. 2013. Influence of humic acid on algal uptake and toxicity of ionic silver. Environ. Sci. Technol. **47:** 8835-8842.

Davies, D. R., and A. Plaskitt. 1971. Genetical and structural analyses of cell-wall formation in *Chlamydomonas reinhardi*. Genet. Res. **17:** 33-43.

De Schamphelaere, K. A. C., C. Nys, and C. R. Janssen. 2014. Toxicity of lead (Pb) to freshwater green algae: development and validation of a bioavailability model and inter-species sensitivity comparison. Aquat. Toxicol. **155:** 348-359.

Eisensamer, B., and T. Roenneberg. 2004. Extracellular pH is under circadian control in *Gonyaulax polyedra* and forms a metabolic feedback loop. Chronobiol. Int. **21:** 27-41.

Errécalde, O., and P. G. C. Campbell. 2000. Cadmium and zinc bioavailability to *Selenastrum capricornutum* (Chlorophyceae): Accidental metal uptake and toxicity in the presence of citrate. J. Phycol. **36:** 473-483.

Errécalde, O., M. Seidl, and P. G. C. Campbell. 1998. Influence of a low molecular weight metabolite (citrate) on the toxicity of cadmium and zinc to the unicellular green alga *Selenastrum capricornutum*: An exception to the free-ion model. Wat. Res. **32:** 419-429.

Fortin, C., and P. G. C. Campbell. 2000. Silver uptake by the green alga *Chlamydomonas reinhardtii* in relation to chemical speciation: Influence of chloride. Environ. Toxicol. Chem. **19:** 2769-2778.

---. 2001. Thiosulfate enhances silver uptake by a green alga: Role of anion transporters in metal uptake. Environ. Sci. Technol. **35:** 2214-2218.

François, L., C. Fortin, and P. G. C. Campbell. 2007. pH modulates transport rates of manganese and cadmium in the green alga *Chlamydomonas reinhardtii* through non-competitive interactions: Implications for an algal BLM. Aquat. Toxicol. **84:** 123-132.

Gorsuch, J. W., C. R. Janssen, C. M. Lee, and M. C. Reiley. 2002. Special issue: The biotic ligand model for metals - current research, future directions, regulatory implications. Comp. Biochem. Phys. C **133:** 1-343.

Gramlich, A., S. Tandy, E. Frossard, J. Eikenberg, and R. Schulin. 2013. Availability of zinc and the ligands citrate and histidine to wheat: Does uptake of entire complexes play a role? J. Agr. Food Chem. **61:** 10409-10417.

---. 2014. Diffusion limitation of zinc fluxes into wheat roots, PLM and DGT devices in the presence of organic ligands. Environ. Chem. **11:** 41-50.

Hinsinger, P., C. Plassard, C. X. Tang, and B. Jaillard. 2003. Origins of root-mediated pH changes in the rhizosphere and their responses to environmental constraints: A review. Plant Soil **248:** 43-59.

Hudson, R. J. M. 1998. Which aqueous species control the rates of trace metal uptake by aquatic biota? Observations and predictions of non-equilibrium effects. Sci. Tot. Environ. **219:** 95-115.

Kola, H., L. M. Laglera, N. Parthasarathy, and K. J. Wilkinson. 2004. Cadmium Adsorption by *Chlamydomonas reinhardtii* and its Interaction with the Cell Wall Proteins. Environ. Chem. **1:** 172-179.

Kühn, S. F., and J. A. Raven. 2008. Photosynthetic oscillation in individual cells of the marine diatom *Coscinodiscus wailesii* (Bacillariophyceae) revealed by microsensor measurements. Photosynth. Res. **95:** 37-44.

Lamelas, C., and V. I. Slaveykova. 2008. Pb uptake by the freshwater alga *Chlorella kesslerii* in the presence of dissolved organic matter of variable composition. Environ. Chem. **5:** 366-372.

Lamelas, C., K. J. Wilkinson, and V. I. Slaveykova. 2005. Influence of the composition of natural organic matter on Pb bioavailability to microalgae. Environ. Sci. Technol. **39:** 6109-6116.

Lavoie, M., J. Bernier, C. Fortin, and P. G. C. Campbell. 2009a. Cell homogenization and subcellular fractionation in two phytoplanktonic algae: Implications for the assessment of metal subcellular distributions. Limnol. Oceanogr.-Meth. **7:** 277-286.

Lavoie, M., S. Le Faucheur, C. Fortin, and P. G. C. Campbell. 2009b. Cadmium detoxification strategies in two phytoplankton species: Metal binding by newly synthesized thiolated peptides and metal sequestration in granules. Aquat. Toxicol. **92:** 65-75.

Liu, F., C. Fortin, and P. G. C. Campbell. 2017. Can freshwater phytoplankton access cadmium bound to low-molecular-weight thiols? Limnol. Oceanogr.**:** doi: 10.1002/lno.10593.

Macfie, S. M., Y. Tarmohamed, and P. M. Welbourn. 1994. Effects of cadmium, cobalt, copper, and nickel on growth of the green alga *Chlamydomonas reinhardtii*: The influences of the cell wall and pH. Arch. Environ. Cont. Toxicol. **27:** 454-458.

Martell, A. E., and R. M. Smith. 2004. NIST Critically Selected Stability Constants of Metal Complexes v. 8.0. NIST Standard Reference Data Base 46. National Institute of Standards and Technology.

Milligan, A. J., C. E. Mioni, and F. M. M. Morel. 2009. Response of cell surface pH to pCO_2 and iron limitation in the marine diatom *Thalassiosira weissflogii*. Mar. Chem. **114:** 31-36.

Morel, F. M. M. 1983. Trace metals and microorganisms, p. 300-308. Principles and Applications of Aquatic Chemistry. J. Wiley & Sons Ltd.

Motulsky, H., and A. Christopoulos. 2003. Fitting models to biological data using linear and nonlinear regression. A practical guide to curve fitting. GraphPad Software Inc.

Nys, C. and others 2014. Development and validation of a biotic ligand model for predicting chronic toxicity of lead to *Ceriodaphnia dubia*. Environ. Toxicol. Chem. **33:** 394-403.

Panfili, F., A. Schneider, A. Vives, F. Perrot, P. Hubert, and S. Pellerin. 2009. Cadmium uptake by durum wheat in presence of citrate. Plant Soil **316:** 299-309.

Paquin, P. R. and others 2002. The biotic ligand model: A historical overview. Comp. Biochem. Phys. C **133:** 3-35.

Phinney, J. T., and K. W. Bruland. 1994. Uptake of lipophilic organic Cu, Cd, and Pb complexes in the coastal diatom *Thalassiosira weissflogii*. Environ. Sci. Technol. **28:** 1781-1790.

Playle, R. C., R. W. Gensemer, and D. G. Dixon. 1992. Copper accumulation on gills of fathead minnows: Influence of water hardness, complexation and pH of the gill micro-environment. Environ. Toxicol. Chem. **11:** 381-391.

Playle, R. C., and C. M. Wood. 1989. Water pH and aluminum chemistry in the gill micro-environment of rainbow trout during acid and aluminum exposures. J. Comp. Physiol. B **159:** 539-550.

Rüdel, H. and others 2015. Consideration of the bioavailability of metal/metalloid species in freshwaters: experiences regarding the implementation of biotic ligand model-based approaches in risk assessment frameworks. Environ. Sci. Pollut. Res. **22:** 7405-7421.

Sánchez-Marín, P., C. Fortin, and P. G. C. Campbell. 2013. Copper and lead internalisation by freshwater microalgae at different carbonate concentrations. Environ. Chem. **10:** 80-90.

Slaveykova, V., and K. Wilkinson. 2003. Effect of pH on Pb biouptake by the freshwater alga *Chlorella kesslerii*. Environ. Chem. Lett. **1:** 185-189.

Slaveykova, V. I., and K. J. Wilkinson. 2002. Physicochemical aspects of lead bioaccumulation by *Chlorella vulgaris*. Environ. Sci. Technol. **36:** 969-975.

---. 2005. Predicting the bioavailability of metals and metal complexes: Critical review of the biotic ligand model. Environ. Chem. **2:** 9-24.

Wilkinson, K. J., and J. Buffle. 2004. Critical evaluation of physicochemical parameters and processes for modelling the biological uptake of trace metals in environmental (aquatic) systems, p. 445-533. *In* H. P. van Leeuwen and W. Koster [eds.], Physicochemical kinetics and transport at biointerfaces. Wiley.

Worms, I. A. M., J. Boltzman, M. Garcia, and V. I. Slaveykova. 2012. Cell-wall-dependent effect of carboxyl-CdSe/ZnS quantum dots on lead and copper availability to green microalgae. Environ. Pollut. **167:** 27-33.

Zhao, C. M., and K. J. Wilkinson. 2015. Biotic ligand model does not predict the bioavailability of rare earth elements in the presence of organic ligands. Environ. Sci. Technol. **49:** 2207-2214.

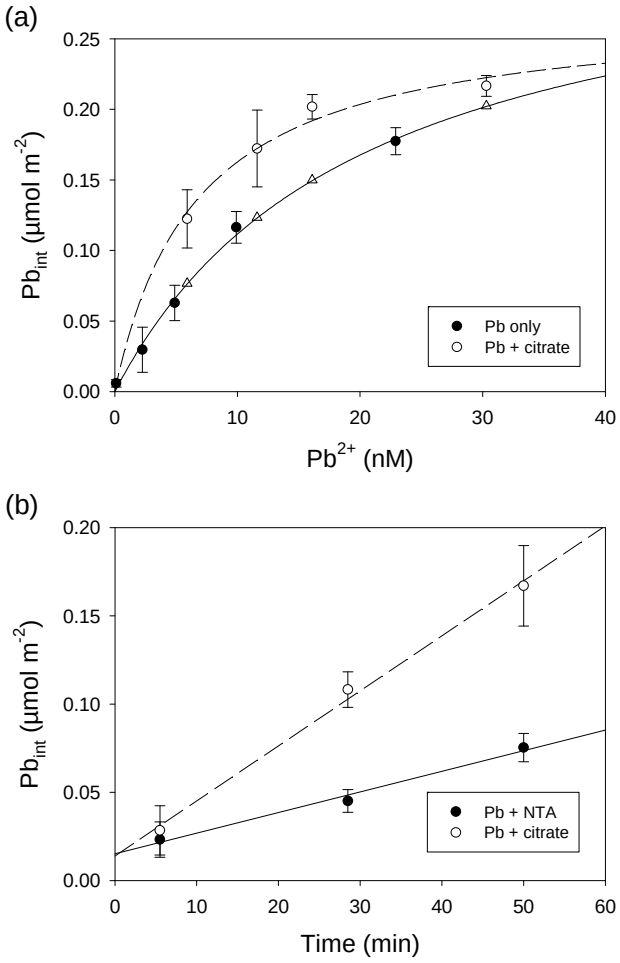

Figure 1. (a) Pb internalized by *Chlamydomonas reinhardtii* CPCC11 (35 min exposure) plotted *vs.* calculated [Pb^{2+}] in the experimental solutions in the absence of added ligands (Pb only) and in the presence of 100 nM Pb_T and added citrate at concentrations ranging from 1×10^{-6} to 1×10^{-5} M (Pb + citrate). (b) Time course of Pb internalization by *C. reinhardtii* exposed to 6.8 nM Pb^{2+} (1 µM Pb_T) in the presence of 1.15 µM NTA (Pb + NTA) or 0.12 mM citrate (Pb + citrate). Lines represent the fitting of the data to the hyperbolic equation (Eqn 1) or to a linear equation. Means ± SD (n = 4–5) are represented. Triangles in (a) represent the predicted Pb internalization considering the sum of Pb^{2+}-dependent internalization and the calculated internalization of Pb-citrate by piggy-back transport (see text for details).

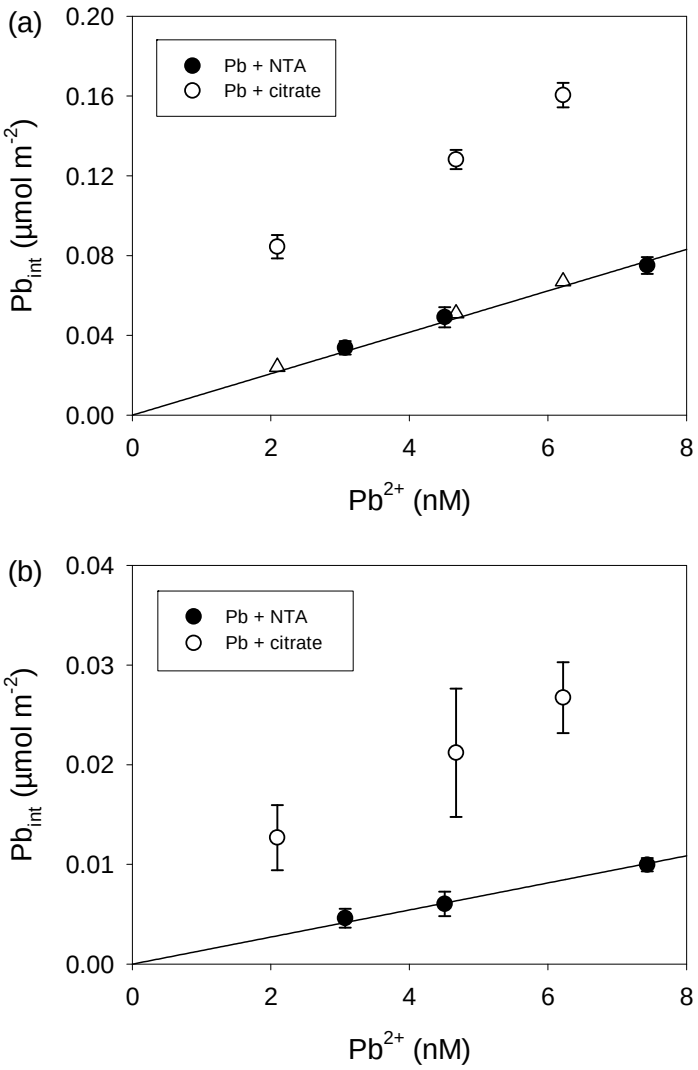

Figure 2. Short-term (35 min) Pb internalization by (a) *Chlamydomonas reinhardtii* wild type CPCC11 or (b) wall-less strain CPCC12 as a function of ISE-measured [Pb^{2+}] in the experimental solutions. Free Pb^{2+} concentrations were buffered with 1.1 to 1.3 µM NTA (black circles) or with 80 to 200 µM citrate (white circles). Total lead concentrations, Pb_T, were 1 µM for all treatments. Lines represent the fitting of the data to a linear uptake model. Means ± SD (n = 3) are represented. Triangles in (a) represent the predicted Pb internalization considering the sum of Pb^{2+}-dependent internalization and the calculated internalization of Pb-citrate by piggy-back transport (see text for details).

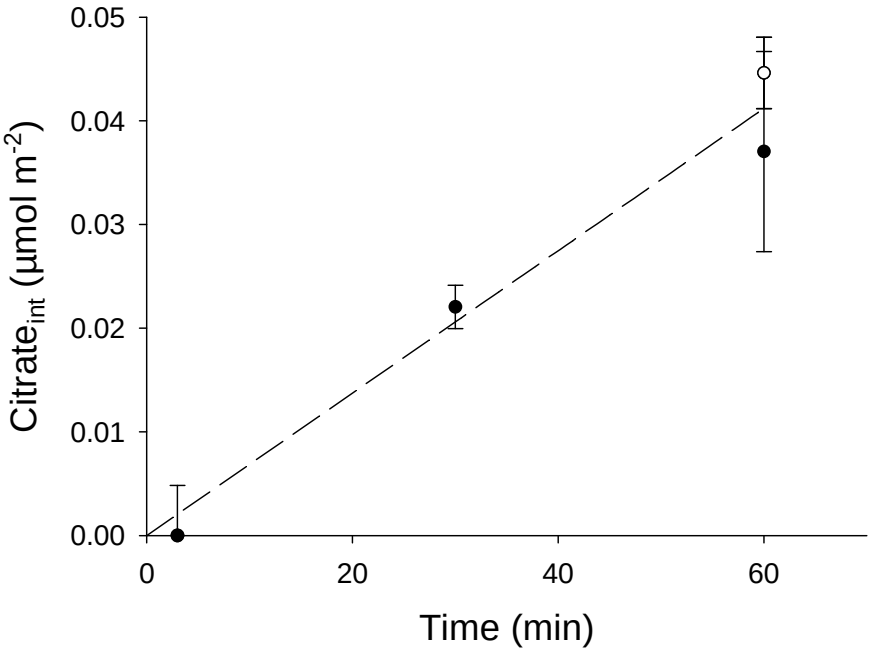

Figure 3. Citrate assimilated by *Chlamydomonas reinhardtii* exposed to 10^{-5} M citrate in the presence (black circles) or absence (white circle) of 100 nM Pb, as a function of exposure time. Citrate assimilation is normalized with respect to the cell surface area. The first time point (3 min) was below the limit of detection (4.8 nmol citrate m^{-2}). Mean values ± SD (n = 2) are represented.

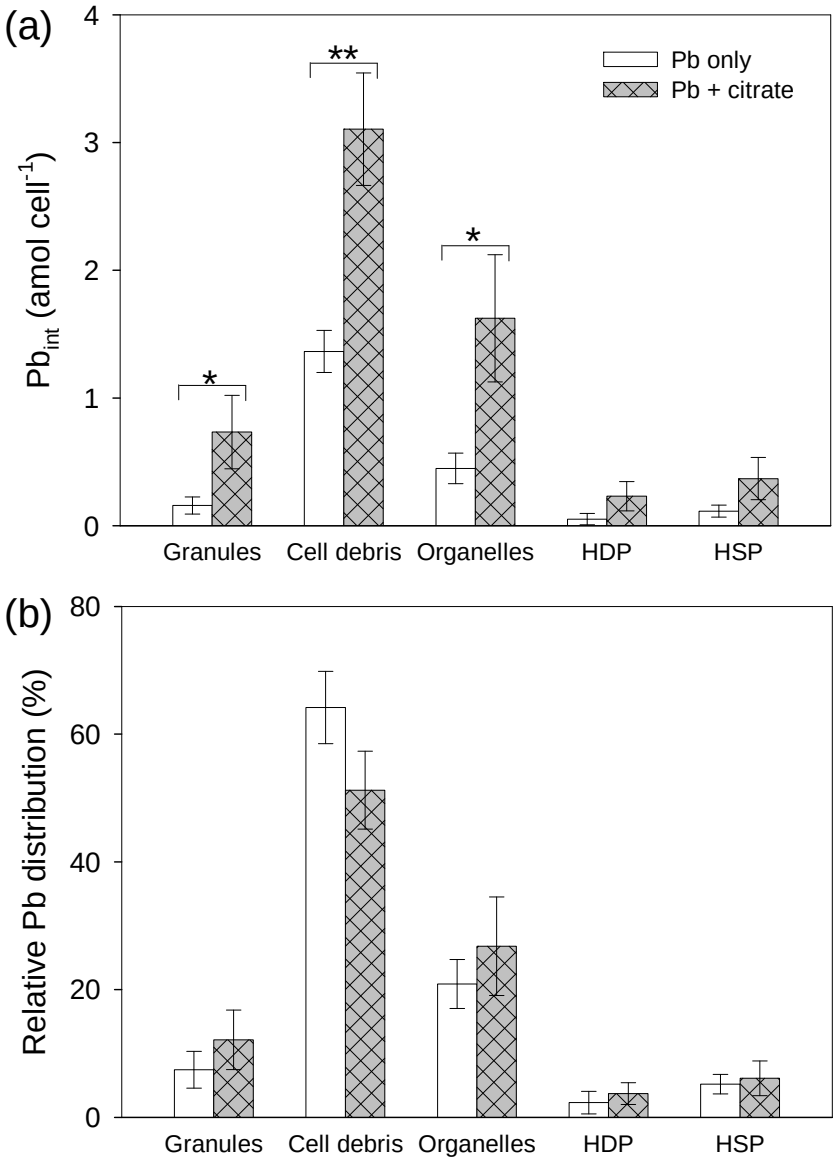

Figure 4. Absolute (a) and relative (b) values of Pb subcellular distribution in *Chlamydomonas reinhardtii* CPCC11 exposed to ~10 nM Pb^{2+} in the absence or presence of 100 μM citrate. HDP = heat-denaturable proteins; HSP = heat-stable proteins. Means ± SD (n = 3) are represented. Significant differences between values in the absence or presence of citrate are represented by * ($p < 0.05$) or ** ($p < 0.01$).

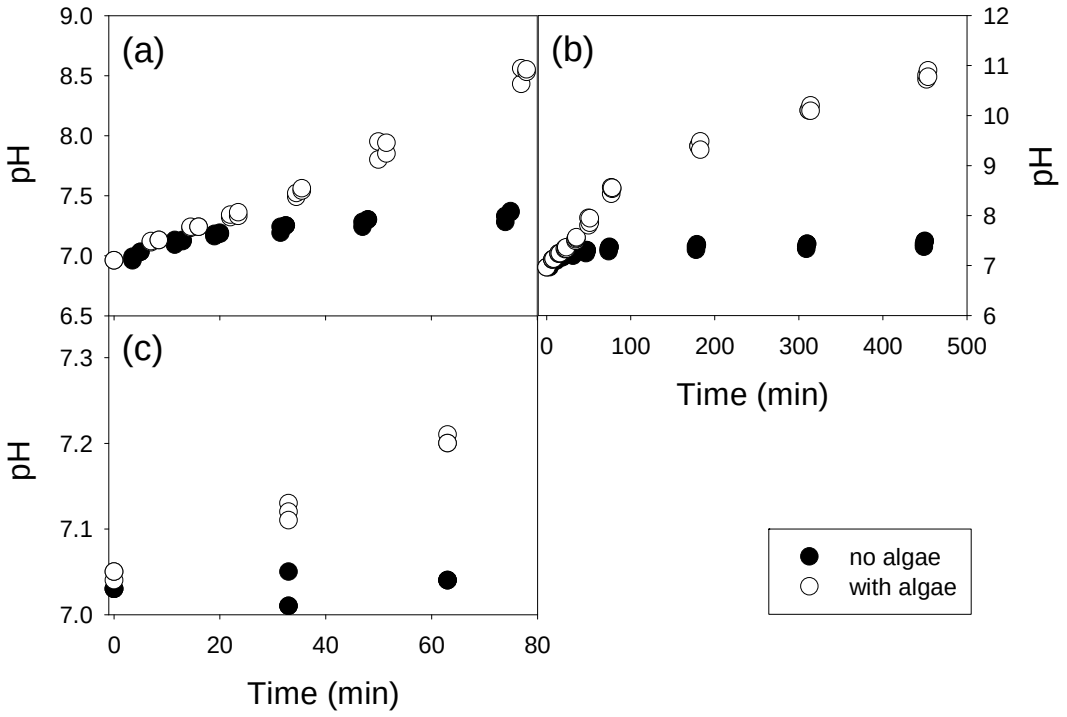

Figure 5. pH increase in the bulk solution (SMHSM with addition of 4 mM $NaHCO_3$) by *Chlamydomonas reinhardtii* CPCC11 at different time scales (a, b) at 5×10^6 cells mL^{-1} in the absence of pH buffer and (c) at 6×10^7 cells mL^{-1} in the presence of 10 mM HEPES. Three replicates are shown.

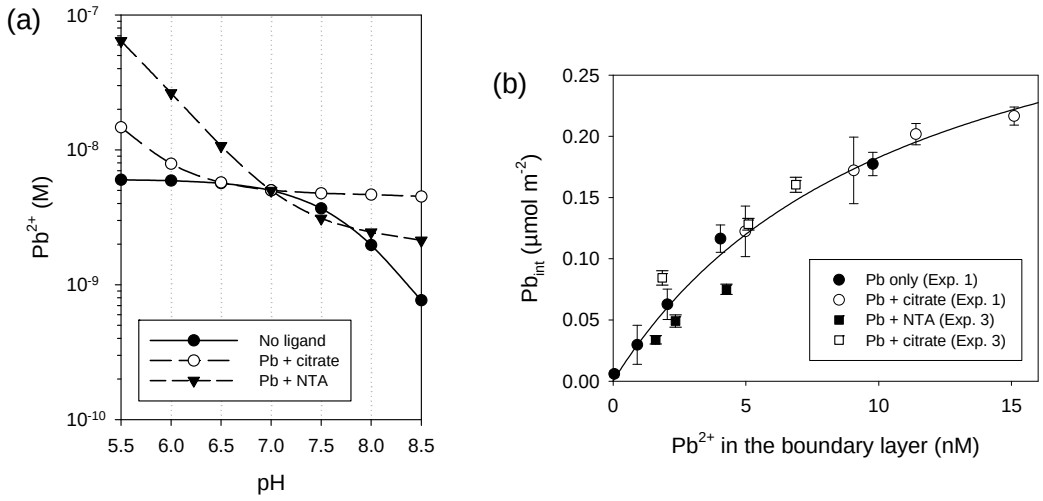

Figure 6. (a). Theoretical variation of Pb^{2+} concentrations at varying pH in solutions designed to have similar Pb^{2+} concentrations at pH 7 in the absence of ligand (6.49 nM Pb_T) or in the presence of 1.19 µM NTA or 0.102 mM citrate (1 µM Pb_T). Medium composition is SMHSM closed to the atmosphere (DIC = 14 µM). Formation of precipitates was not considered in the calculation. (b) Pb internalized by *Chlamydomonas reinhardtii* CPCC11 (35-min exposure) plotted *vs.* calculated [Pb^{2+}] in the boundary layer assuming that the pH changed from 7 to 8. Internalization results correspond to those plotted in Figure 1a (Exp. 1) and 2a (Exp. 3), respectively. The uptake curve was obtained from fitting of all data to Eqn. 1.

Supporting information

Article title:

Microalgal-driven pH changes in the boundary layer lead to apparent increases in Pb internalization by a unicellular alga in the presence of citrate.

Authors:

Paula Sánchez-Marín, Fengjie Liu, Zhongzhi Chen, Claude Fortin and Peter G.C. Campbell

Table of contents:

Table S1. Composition of exposure media in experiment 1, consisting of a 35-min exposure of *Chlamydomonas reinhardtii* CPCC11 to "Pb only" or "Pb + citrate" treatments. Internalization results are shown in Figure 1a.[a]

	Pb only	**Pb + citrate**
Component		
Ca	6.80×10^{-5}	6.80×10^{-5}
Mg	8.12×10^{-5}	8.12×10^{-5}
Na	4.00×10^{-3}	4.00×10^{-3}
NH_4	9.38×10^{-4}	9.38×10^{-4}
NO_3	5.07×10^{-3}	5.07×10^{-3}
SO_4	8.12×10^{-5}	8.12×10^{-5}
Pb	$1.45\times10^{-10} – 3.22\times10^{-8}$	$7.80\times10^{-8} – 9.05\times10^{-8}$
Citrate	-	$1\times10^{-6} – 1\times10^{-5}$
Calculated species		
Pb^{2+}	$1.06\times10^{-10} – 2.29\times10^{-8}$ (71 – 75% of Pb_T)	$5.89\times10^{-9} – 3.03\times10^{-8}$ (6 – 30% of Pb_T)
Ca^{2+}	6.65×10^{-5}	$6.33\times10^{-5} – 6.62\times10^{-5}$
Mg^{2+}	8.06×10^{-5}	$7.64\times10^{-5} – 8.02\times10^{-5}$
Ionic Strength	5.45×10^{-3}	5.45×10^{-3}
pH	6.95 – 7.05	6.95 – 7.01

[a] Dissolved inorganic carbon concentrations derived from atmospheric inputs were *ca*. 1.4×10^{-5} M on the basis of analytical measurements.

Table S2. Composition of exposure media in experiment 2, a determination of the time-course of Pb uptake by *Chlamydomonas reinhardtii* CPCC11 in "Pb + NTA" or "Pb + citrate" media. Internalization results are shown in Figure 1b. [a]

	Pb + NTA	**Pb + Citrate**
Component		
Ca	6.80×10^{-5}	1.10×10^{-4}
Mg	8.12×10^{-5}	1.35×10^{-4}
Na	5.12×10^{-3}	4.17×10^{-3}
NH_4	9.38×10^{-4}	9.38×10^{-4}
NO_3	6.00×10^{-3}	5.75×10^{-3}
SO_4	8.12×10^{-5}	8.12×10^{-5}
Pb	1.01×10^{-6}	1.01×10^{-6}
NTA	1.15×10^{-6}	-
Citrate	-	1.20×10^{-4}
Calculated species		
Pb^{2+}	6.80×10^{-9}	6.79×10^{-9}
Ca^{2+}	6.65×10^{-5}	6.84×10^{-5}
Mg^{2+}	8.06×10^{-5}	8.32×10^{-5}
Ionic Strength	6.50×10^{-3}	6.50×10^{-3}
pH	7.0	7.0

[a] Dissolved inorganic carbon concentrations derived from atmospheric inputs were *ca*. 1.4×10^{-5} M on the basis of analytical measurements.

Table S3. Composition of exposure media in experiment 3, consisting of a 35-min exposure wall-less or walled strains of *Chlamydomonas reinhardtii* to "Pb + NTA" or "Pb + citrate" treatments in pH buffered media. Internalization results are shown in Figure 2. [a]

	Pb + NTA	**Pb + citrate**
Component		
Ca	6.80×10^{-5}	6.80×10^{-5}
Mg	8.12×10^{-5}	8.12×10^{-5}
Na	6.33×10^{-3}	6.45×10^{-3} – 6.88×10^{-4}
NH_4	9.38×10^{-4}	9.38×10^{-4}
NO_3	5.07×10^{-3}	5.07×10^{-3}
SO_4	8.12×10^{-5}	8.12×10^{-5}
Pb	1×10^{-6}	1×10^{-6}
NTA	1.1×10^{-6} – 1.3×10^{-6}	-
Citrate	-	8×10^{-5} – 2×10^{-4}
HEPES	1×10^{-2}	1×10^{-2}
Calculated species		
Pb^{2+}	3.46×10^{-9} – 9.30×10^{-9}	2.06×10^{-9} – 7.42×10^{-9}
Ca^{2+}	6.65×10^{-5}	2.31×10^{-5} – 4.38×10^{-5}
Mg^{2+}	8.06×10^{-5}	2.68×10^{-5} – 5.19×10^{-5}
Ionic Strength	6.6×10^{-3}	6.7×10^{-3} – 7.1×10^{-3}
pH	6.97	6.95

[a] Dissolved inorganic carbon concentrations derived from atmospheric inputs were *ca*. 1.4×10^{-5} M on the basis of analytical measurements.

Table S4. Comparison of internalized citrate with the "extra" Pb internalized by *Chlamydomonas reinhardtii* wild type (i.e., above BLM predictions) after 35-min exposure to different Pb and citrate concentrations.

Medium composition[a]				*Pb/citrate internalization*			
Pb_T (µM)	*Citrate* (µM)	Pb^{2+} (nM)	$Pbcit^{1-}$ (nM)	*Observed* Pb_{int} (µmol m^{-2})	*Observed extra-*Pb_{int} (µmol m^{-2})	*Calculated* $citrate_{int}$ (µmol m^{-2})	*Ratio* $citate_{int}$ / *extra-*Pb_{int}
0.1	1	30.3	37.2	0.217	0.015	0.002	0.17
0.1	3	16.1	60.6	0.202	0.052	0.007	0.14
0.1	5	11.6	74.5	0.172	0.049	0.012	0.25
0.1	**10**	**5.89**	**77.1**	**0.122**	**0.046**	**0.024 ± 0.002**[b]	**0.53**
1	80	7.42	990	0.161	0.096	0.20	2.0
1	100	5.52	992	0.128	0.079	0.25	3.1
1	200	2.06	996	0.084	0.059	0.49	8.3

[a] Nominal concentrations.

[b] Citrate uptake value was determined experimentally at identical citrate concentrations (n = 3). The other uptake values in this column were calculated, with the assumption that uptake was a linear function of [citrate].

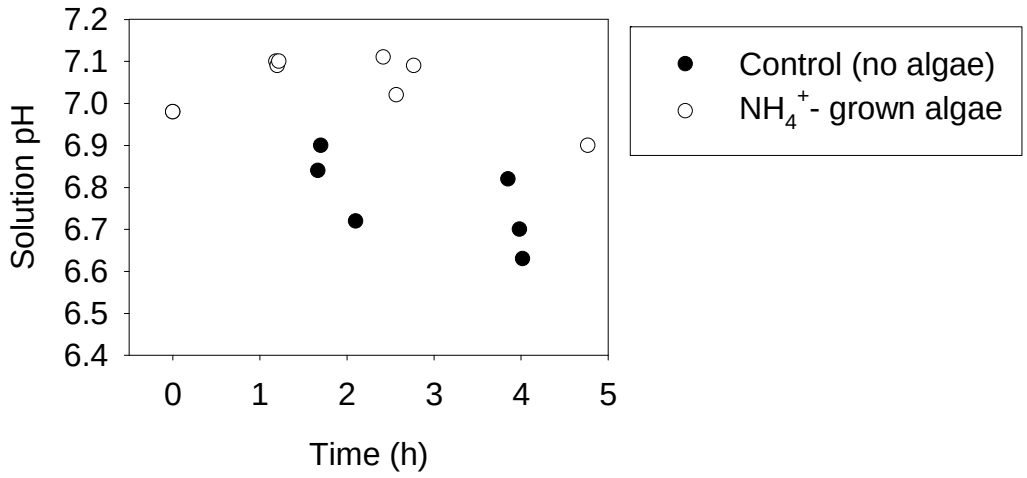

Figure S1. Change in pH of SMHSM solution after adding *C. reinhardtii* CPCC11 at high cell density (1.3×10^6 cells mL^{-1}) compared to that in a control solution in the absence of algae. The solutions were sealed in 50-mL centrifuge tubes without head space and incubated at 20 ºC and constant light (100 µmol photons m^{-2} s^{-1}). The small decrease in pH in the absence of algae was likely due to CO_2 exchange with the atmosphere during the pH measurements.

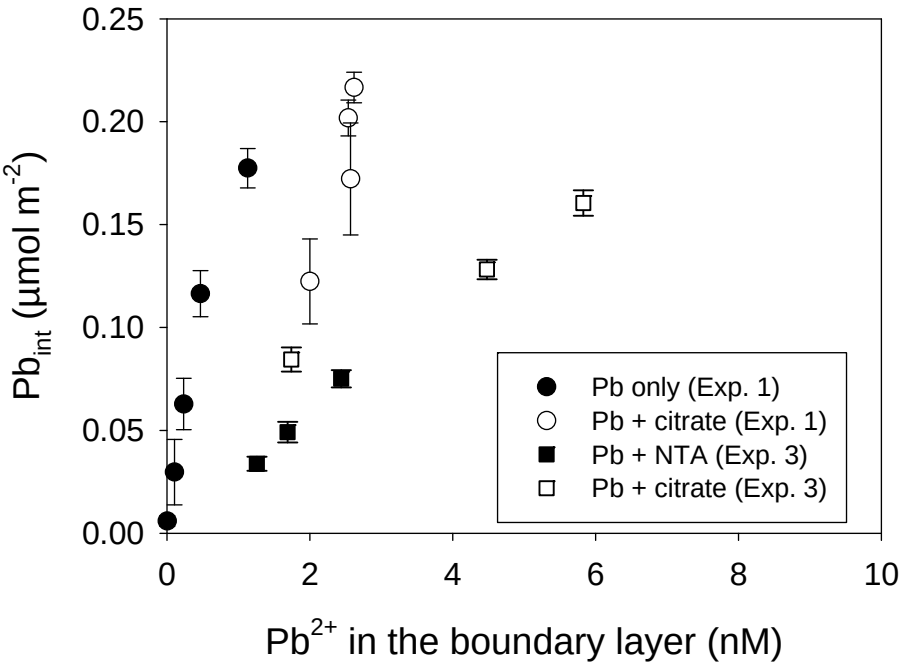

Figure S2. Pb internalized by *Chlamydomonas reinhardtii* CPCC11 (35-min exposure) plotted *vs.* calculated [Pb^{2+}] in the boundary layer assuming that the pH changed from 7 to 9. Recalculation of data presented in Figure 6b.

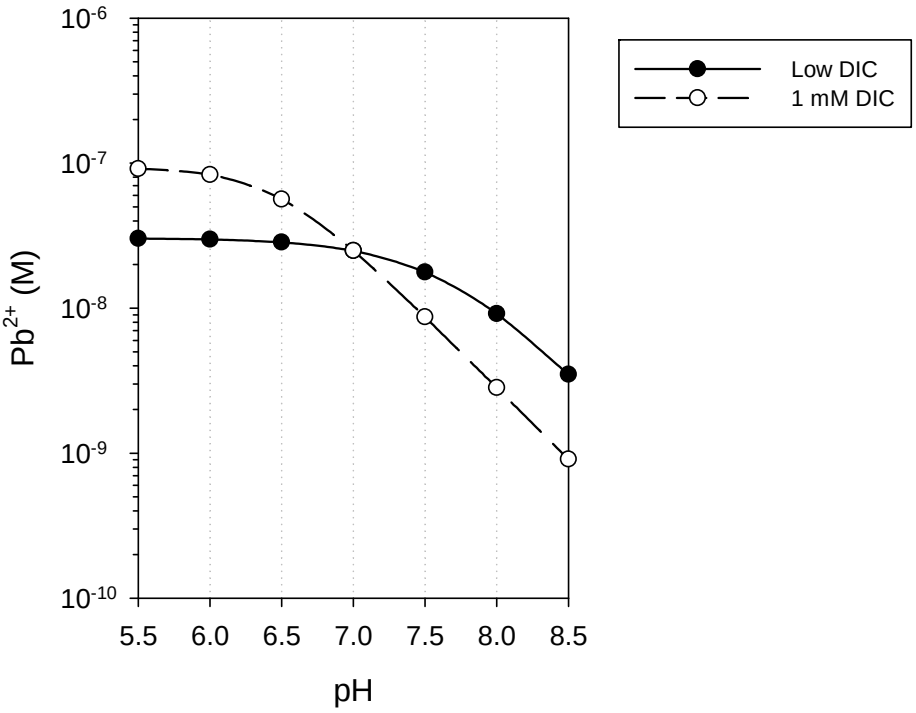

Figure S3. Theoretical variation of Pb^{2+} concentrations at varying pH in solutions designed to have similar Pb^{2+} concentrations at pH 7 in the absence of added CO_3^{2-} (14 µM DIC, 32.7 nM Pb_T) or in the presence of 1 mM DIC (100 nM Pb_T). Medium composition is SMHSM. Simulations were run for solutions closed to the atmosphere and formation of precipitates was not considered in the calculation.

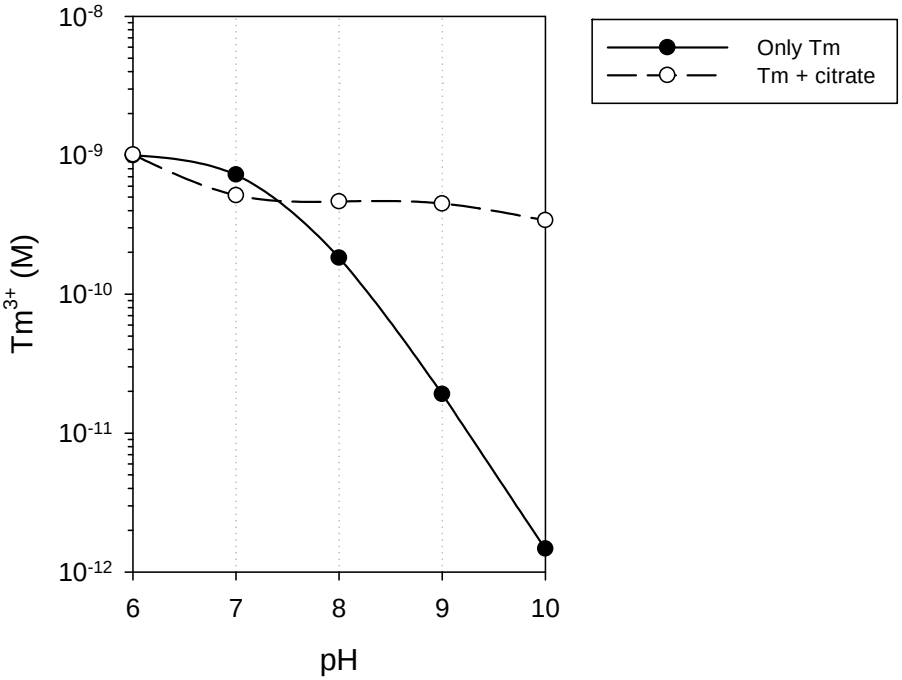

Figure S4. Theoretical variation of Tm^{3+} concentrations at varying pH in solutions designed to have similar Tm^{3+} concentrations at pH 6 in the absence of ligand (1.03 nM Tm_T) or in the presence of 6.5 µM citrate (1 µM Tm_T). Medium composition is the same as described in Zhao and Wilkinson (2015). Simulations were run for solutions closed to the atmosphere (DIC = 14 µM) and formation of precipitates was not allowed.

Reference cited in the Supporting information:

Zhao, C.M. and Wilkinson, K.J., 2015. Biotic ligand model does not predict the bioavailability of rare earth elements in the presence of organic ligands. Environ. Sci. Technol. 49: 2207-2214.